Original Research Article

A promising Ternary Solid Dispersion of Aceclofenac Containing Tablet with Enhanced Dissolution, and Potentiated Anti-inflammatory Efficacy Superlative to Bristaflam.

Abstract:

The major objective of the current study is to implement a plane to enhance the dissolution rate and oral bioavailability of a poorly water-soluble aceclofenac. The drug is classified according to biopharmaceutical classification system as class II drug. Amorphous alkalinized aceclofenac solid dispersion were formulate as a ternary mixture. This mixture was prepared by introducing polymeric carriers [polyvinylpyrrolidone, Hydroxy propyl beta cyclodextrin or Polyethylene glycol] and an alkalizer (Na_2CO_3) by applying solvent evaporation method. Optimum formulations were compressed into tablets that subjected to in-vitro studies compared to market product Bristaflam and free drug containing one. Finally, tablets were assessed for stability studies and carrageenan-induced rat paw edema treatment to evaluate potentiated anti-inflammatory efficacy.

Results showed that optimum amorphous alkalinized aceclofenac solid dispersion formulations containing polyvinylpyrrolidone K30 or Hydroxy propyl beta cyclodextrin in 1:5 ratio have significant in-vitro dissolution improvement (>90% in 10 min) compared to untreated aceclofenac. Solid-state characterization emphasized the conversion of crystalline drug into the amorphous form with no drug−polymers interactions. Stability and dissolution studies ensured that tablets containing amorphous alkalinized solid dispersions were stable with strikingly improving in dissolution behavior compared to Bristaflam or free drug containing tablets. Moreover, regarding anti-inflammatory activity against carrageenan induced paw edema, and histopathological examination, we concluded that amorphous

alkalinized solid dispersions containing tablets are promising approach to enhance the dissolution rate and oral bioavailability and hence anti-inflammatory efficacy of aceclofenac.

Keywords: Aceclofenac, solid dispersion containing tablets, polymeric carrier, alkalizer, Anti-inflammatory efficacy.

1. INTRODUCTION

Approximately 40% of active pharmaceutical ingredients (API) developed by the pharmaceutical industry and 90% of drugs in the development pipeline are poorly water-soluble [1]. There have been various effective approaches used to improve the solubility, dissolution, and bioavailability of these drugs [8-2]. Some of the most prevalent approaches are reduction in particle size (micronization, nanosizing) [9], cyclodextrin drug complexation [10], lipid based formation [11], using of surfactant [12], formation of a salt with alkalizing agent [13], and using different alkalizers in SD to change the pH of the microenvironment [14]. Among these, incorporation of alkalizing agents in a SD has been identified as an effective method for increasing the dissolution rate of water-insoluble drugs [15].

Solid dispersion (SD) technology has been routinely utilized to enhance the dissolving of poorly soluble drugs [16, 17]. It is typically made by dispersing a hydrophobic drug into biologically nontoxic hydrophilic carriers like polyvinylpyrrolidone (PVP), polyvinylalcohol (PVA), polyethylene glycol (PEG), and hydroxypropyl methylcellulose (HPMC), or surfactants like pluronics, d-tocopheryl polyethylene glycol 1000 succinate (TPGS), and sodium dodecyl sulphate (SDS), using various techniques such as spray drying, lyophilization, solvent evaporation, and hot melt extrusion [18]. A crystalline substance is commonly transformed into an amorphous form in SDs [19, 20]. As a result, the drug's solubility was improved, resulting in better oral absorption. Hydrophilic carriers are critical for improving drug wettability and maintaining the super-saturable state [21]. Aceclofenac (AFC) (2-[(2,6-dichlorophenyl) amine] phenylacetoxyacetic acid) is a new generational non-steroidal anti-inflammatory drug (NSAID) that is thought to be a better option to diclofenac and other NSAIDs in term of gastrointestinal safety [22, 23]. The fundamental issue with AFC's therapeutic response in an orally administered dose form is its low water solubility, as it is a biopharmaceutical classification system (BCS) Class II [23-26].

The objective of this study was to modulate the dissolution behavior, improve oral bioavailability and hence the anti-inflammatory efficacy of the weak acidic drug AFC applying alkalizer polymeric SD system. Based on dissolution test results, the optimum formulations were selected, characterized, compressed into tablets using microcrystalline cellulose (MCC) as a directly compressible vehicle then subjected to stability study and assessed for carrageenan-induced rat paw edema treatment.

2. MATERIAL AND METHODS

AFC and PEG 6000 were purchased from Alfa easer (Germany). Hydroxypropyl beta cyclodextrin (HPβCYD) was purchased from Loba Chemie Pvt Ltd (India). PVP k30 was purchased from sigma- Aldrich (USA). Sodium carbonate, di-sodium hydrogen orthophosphate and sodium bicarbonate were purchased from El Nasr pharmaceutical chemicals co (Egypt). Potassium hydroxide and MCC were purchased from S D Fine-Chem Limited (Mumbai, india). Other chemicals were of analytical grade.

2.1. Solubility study

AFC solubility was found out in various media (distilled water, phosphate buffer pH 6.8 and 1% w/v solutions of several alkalizes Na_2CO_3, $NaHCO_3$, Na_2HPO_4 and KOH). An extra amount of AFC was dropped to test tubes with screw caps and maintained for three days in a shaking water bath thermostatically controlled (Grant Instrument Cambridge Ltd., Barrington Cambridge (B2, 5002, England) at a temperature of 37 ±0.5 then left for equilibrium one day. A suitable volume of supernatant

from each tube was taken, filtered through 0.45 µm membrane filter, diluted to an acceptable concentration and analyzed spectrophotometrically (UV/VIS spectrophotometer (JASCO, V-530, Japan) at 276 nm. All the experiments were triplicated.

2.2. Preparation of amorphous alkalinized aceclofenac solid dispersion (AA-AFC-SD) formulations and Physical Mixtures (PMs):

AA-AFC-SDs were made utilizing solvent evaporation process by employing three various polymers (PVP K30, PEG 6000, HPβCYD) with a drug to polymer ratio 1:1, 1:3 and 1:5 respectively as mentioned in Table 1. Na_2Co_3 was added as a selected alkalizer based on the solubility study. It was maintained by a ratio of 1:6 (Na_2Co_3: AFC) in all formulations. Ternary mixture was prepared by adding 1 g of AFC and 167 mg of Na_2Co_3 to distilled water, stirring for about 30 min at room temperature until reaching a clear solution. Mixing each polymer with the clear solution by their respective ratios mentioned before till reaching a uniform mixture. The mixture allowed to evaporate in a vacuum pump. The obtained residue was collected and stored for further use. Each PM was obtained by mixing a suitable amount of AFC, Na_2Co_3 by a ratio of 6:1 and one of the three different polymers (PVP K30, PEG 6000, HPβCYD) with their respective ratios mentioned before until a uniform mixture was reached using mortar and pastel, stored in a room temperature 25 ^{O}C for further use [15].

Table 1: Composition of Aceclofenac formulations

Formula code		Polymer used	(Drug: Polymer) Ratio
Solid dispersion	Physical mixture		
SD1	PM1	PVP K30	1:1
SD2	PM2	PVP K30	1:3
SD3	PM3	PVP K30	1:5
SD4	PM4	PEG 6000	1:1
SD5	PM5	PEG 6000	1:3
SD6	PM6	PEG 6000	1:5
SD7	PM7	HPβCYD	1:1
SD8	PM8	HPβCYD	1:3
SD9	PM9	HPβCYD	1:5

Notes: *Na_2CO_3 ratio was fixed in all formulation 1:6 (Na_2Co_3: AFC).*
Abbreviations: *SD, solid dispersion; PM, physical mixture; PVP K30, polyvinylpyrrolidone k30; PEG 6000, polyethylene glycol 6000; HPβCYD, hydroxy propyl beta cyclodextrin.*

2.3. Solid-state characterization

The following approaches were used to characterize pure AFC, Na_2Co_3, and carriers (PVP K30 and HPβCYD), as well as the optimized AA-AFC-SDs and their associated PMs, in the solid state**.**

2.3.1. Fourier-transform infrared spectroscopy (FTIR).

Compressed discs of 2 mg for each sample crushed with 200 mg potassium bromide and used to acquire the (FTIR) spectra (Thermo Fisher Scientific) of the investigated materials. Disks were scanned in the 500–4,000 cm^{-1}wavenumber range. Each sample's FTIR spectra was obtained by recording distinctive bands [27].

2.3.2. Differential scanning calorimetry (DSC).

Using DSC apparatus (TA Instruments, SDTQ600, New Castle, USA) and nitrogen atmosphere at a flow rate of 30 ml min^{-1}, DSC measurements were performed using 4 mg of each sample in an aluminum pan and subjected to a temperature range of 25–500 □ C and heating rate of 10 ^{O}C min^{-1}.

2.3.3. X-ray diffractometry (XRD).

A diffractometer prepared with CoK (Diano, Woburn, MA, USA) was used to obtain XRD patterns at 45 kV, 9 mA, and 2θ angle [27].

2.3.4. Scanning electron microscopy (SEM).

SEM was used to evaluate the morphological properties of pure AFC, it's prepared SDs, and related PMs (SEM; JSM 5500 LV; JEOL, Tokyo, Japan). On a SEM holder, the samples were dispersed and sticky tape with two sides was used to fix them. A sputter coater (S-150A; Edwards, Crawley, UK) working in a for 2 minutes a vacuum (3×10-1 atm) of Argon gas was utilized to cover the sample that has been fixed with a film of gold of 150 °A [27].

2.3.5. Percentage yield:

Each SD's dry residue was accurately weighed, and the percentage yield was calculated using this equation [28, 29].

$$\% \text{ yield} = \frac{wieght\ of\ dried\ residue.}{weight\ of\ AFC + Na2Co3 + polymer\ used} \times 100$$

2.3.6. Drug content

An amount of each SD equivalent to 10 mg of AFC was added to 25 ml methanol in a volumetric flask, diluted to a suitable concentration and measured spectrophotometrically at 276 nm. All estimations were triplicated [30]. The following equation was used to calculate the actual drug content:

$$\% \text{ Drug content} = \frac{the\ actual\ drug\ content.}{the\ theoritical\ drug\ contet} \times 100.$$

2.4. In-vitro dissolution rate analysis.

Analysis of dissolution rate was observed in 900 ml phosphate buffer (pH 6.8) applying USP apparatus (paddle method) (Dissolution Apparatus USP Standards, Scientific, DA-6D, Bombay, India) maintained at 50 rpm and 37±0.5 °C. Pure 100 mg AFC, each SDs, and PMs having an equivalent amount of 100 mg AFC were exposed to dissolution test for 2 hr. One ml from the media was pulled up at fixed time intervals 10, 20, 30, 45, 60, 90, 120 mints, then compensated with 1 ml of the fresh media. Samples were filtered through 0.45 µm membrane filter, allowed for convenient dilution with the fresh media and measured spectrophotometrically at 276 nm .All the analysis study was achieved in triplicate [31]. The area beneath the curve of dissolution at time (T) was compared to that of a rectangle described by 100 % dissolution at the same time to compute

dissolution efficiency (DE) [32, 33]. The relative dissolution rate (RDR) was calculated by comparing the percentage dissolved AFC from either ternary system (SDs or PMs) to that of the drug alone [33, 34].

2.5. Pre-formulation studies.

Angle of repose, Carr's index (Compressibility index), and Hausner's ratio were used to assess the flow properties of the powder blend (optimized SDs and Microcrystalline cellulose MCC) prior to compression. The tapped and bulk densities were used to estimate the last two values [35].

2.5.1. Angle of repose.

The drained angle of repose of the powder combination was determined using the fixed funnel and free-standing cone method. The procedure involved fixing a funnel with its tip at a specific height, h, which was kept 2 cm above graph paper on a flat horizontal surface**.** Excess quantities of each mixture were allowed to drain above a given diameter base until a cone of powder formed on the fixed diameter, where r is the radius of the conical pile base. The angle of repose θ can be calculated using the equation [36].

$$\theta = \tan^{-1}\frac{h}{r}$$

***2.5.2.* Bulk and Tapped Densities.**

A predefined weight equivalent to 5 g of the powder blend was poured into a graduated estimating cylinder to determine apparent bulk density (B_d). The bulk volume (B_v) was observed. The following equation was used to compute bulk density [35].

$$\text{Bulk density } (B_d) = \frac{wieght\ of\ the\ powder\ blend\ (5\ gm)}{bulk\ volume\ of\ bowder\ blend}$$

The tapping was then kept going until the volume had remained unchanged, and the observed volume was verified as tapped volume. The following equation was used to calculate the tapped density [36].

$$\text{Tapped density } (T_d) = \frac{wieght\ of\ the\ powder\ blend\ (5\ gm)}{tapped\ \ volume\ of\ bowder\ blend}$$

***2.5.3.* Compressibility index.**

Compressibility index was calculated using the equation below [26].

$$\text{Compressibility index} = \frac{Td - Bd}{Td} x\ 100$$

***2.5.4.* Hausner's ratio.**

The Hausner's ratio values were determined by the formula given below [26].

$$\text{Hausner's ratio} = Td/Bd$$

2.6. Preparation of aceclofenac containing tablets:

Each optimized SD formulae was mixed by a portion of 69.7% with 30.1% MCC as a directly compressible vehicle, then it was additionally tableted by direct compression using a single punch tablet press (Erweka- Apparatebau, GmbH, E.K.O., West-Germany) as mentioned in [35-37].

2.7. Tablet evaluation.

All of the tablets were tested using both pharmacopeial and non-pharmacopeial methods. Weight consistency by Electric balance (Sartorius TE 2145, Germany), thickness by micrometre (Mitutoyo Corporation, Japan), hardness by Erweka hardness tester (Erweka, GmbH, Germany), friability by Roche friabilator (Erweka, GmbH, Germany), drug content uniformity (Reichal et al. 2011), and drug release are among the tests performed [36].

2.7.1. In-vitro release testing.

Test for in vitro dissolution was done for the prepared tablets compared with free drug containing tablet T5 and commercial one (Bristaflam SmithKline Beecham - Egypt L.L.C. An affiliated Co. to GlaxoSmithKline) by introducing 900 ml phosphate buffer pH (6.8) based on USP II basket method at 37±0.5 °C and 50 rpm, three ml were pulled up at each time interval 10, 20, 30, 45, 60, 90 and 120 mint (equivalent fresh medium volume was added to maintain sink condition), filtered through 0.45 µm membrane filter, diluted to suitable dilution and analyzed spectrophotometrically at 276 nm. This study was done in a triplicate [30].

2.7.2. Release kinetics.

In order to understand the drug-release process, in vitro release data were fitted mathematically using different kinetic models such as; zero order, first order, Higuchi diffusion, and Korsmeyer– Peppas semiempirical. The choice of the superior model was dependent on the kinetic release profile that conveying the highest coefficient (R^2) using GraphPad Prism software version 8.00. Each experiment was repeated in triplicate and the mean was employed.

2.7.3. Stability study.

For the prepared AA-AFC-SD containing tablets, an accelerated stability study following ICH recommendations was used to assess physical changes, drug content, and drug release during storage. Tablets of the selected formulations were put in airtight amber glass bottles and stored for 6 months at room temperature (25± 2□C/40 ±5% relative humidity RH). Others were placed in desiccators containing saturated sodium chloride solutions to produce humidity (RH 75 %±5%) and stored in a thermostatically controlled hot air oven at (40 ±2□C) and (50 ±2□C) for the same period of time for accelerated stability testing. Tablets were tested at the start and at predetermined intervals (3 and 6 months) [36].

2.7.4. Anti-inflammatory activity and therapy of rats with carrageenan-induced paw edema.

Animal protocol was accepted by the ethical committee of Mansoura University's Faculty of pharmacy, Mansoura, Egypt, in accordance with “principles of laboratory animal care NIH publication revised 1985” (Code number: 2022-179)

Moreover, the study was conducted under careful considerations of the Animal Research: Reporting of in vivo Experiments (ARRIVE) guidelines. The animals were maintained in 12 hours of light–12 hours of darkness at 25 ±1°C and 55±5 % RH. They had full entrance to the lab's food and water. Doses were adjusted to suit the body weight of the rats in order to be administered safely [38]. The following equation suggested by Osman and Atya [(39)] was used to downscale the improved formulation.

Animal dose (per 200 g body weight) =Human dose x $\frac{18}{1000}$

Thirty-six healthy male Wistar rats each one weighing about 180–200 g were separated into six groups of six rats each to test the anti-inflammatory properties of the prepared AA-AFC-SD containing tablets in comparison to the free drug containing

tablet and market one, in addition, there were normal and positive control groups. Saline solution was given to group I. (Normal control, 0.1 mL). In the second group of rats 0.1 mL of (1 %w/v) λ-carrageenan in saline were injected into the right hind paw's subplantar region (positive control). Free drug containing tablet (AFC 10 mg/kg) was given orally to group III thirty minutes prior to the injection of carrageenan into the right hind paw. In addition, pretreatment with commercial tablet was given to group IV. Group V and VI were pretreated with AA-AFC-SD containing tablets (T1 and T2 respectively) equivalent to 10 mg/kg AFC thirty minutes prior to the injection of carrageenan into the right hind paw [27]. Measurements of the injected hind paw's volume were performed using plethysmography before and after injection of carrageenan at intervals of 0.5, 1, 2, 3, 4, 5, 6, 7, 8, 12, 24 and 24. Each group's edema and edema suppression were calculated [40].

Edema (E) % = $\frac{Vt-Vo}{Vo}$ x 100

Edema inhibition % = $\frac{Ec-Et}{Ec}$ x100

Where V_o and V_t represent the mean paw volume before and after carrageenan injection at time t, respectively, and E_c and E_t represent the edema percentages of the control and treated groups at the same time interval.

The animals were sacrificed at the termination of the experiment (24 hours), and thin and thick skin samples in the region of the animals' paw were detached. Buffered formalin at 10% (v/v) were used to fix the samples and then treated as usual till histopathological investigation with paraffin embedding [27].

2.7.5. Histopathological examination.

Paraffin blocks with consecutive paw-skin segments (thin and thick) were produced and treated before being stained with hematoxylin eosin (H&E) and seen under a microscope (Leica Microsystems, Wetzlar, Germany) [41]. The grade zero (0) indicates no inflammatory cells, 1 indicates inflammatory cells under 10%, 2 indicates inflammatory cells 10 %–50 %, and 3 indicates inflammatory cells greater than 50% were used to rate the strength of the inflammatory response in each animal's thin- and thick-skin samples. All of this is in relation to the cell population [42]. A pathologist performed all of the readings blindly.

2.7.6. Statistical analysis.

The data was analyzed using a one-way ANOVA followed by Tukey–Kramer multiple-comparison tests. The software used was GraphPad Prism version 8.00 (GraphPad software, San Diego, CA, USA). Differences were considered statistically significant at the level $P<0.05$.

3. RESULTS AND DISCUSSION

3.1. Drug solubility study and choosing of an alkalizing agent for AA-AFC-SD preparations:

AFC has a pH dependent solubility which increased in alkaline medium more than acidic pH [23, 43, 44]. The results indicated that AFC had the greatest solubility in 1% Na_2Co_3 solution (60.515±2.12 mg/ml), so it was chosen as an alkalizing agent for AA-AFC-SD preparations. Alkalizing agent was applied to achieve adequate alkalinity by a ratio of (1:6 for Na_2Co_3: AFC respectively). Similar outcomes have been published. For instance, using alkalizers and polymers in a nanoemulsifying system for dissolution enhancement of AFC [44]. Altering the microenviromental pH by using an alkalizer for increasing AFC solubility and decreasing in-vivo gastrointestinal bleeding [23]. AFC dissolution rate was increased to nearly 100% using immediate release solid dispersions containing the pH modifier [45]. Moreover using various types of polymers, the

crystallinity of the drug was modified into an amorphous state during the preparation of solid dispersions, and pH of the microenvironment was regulated by Na_2Co_3 as a pH modifier, which improved solubility [30].

3.2. Solid-state characterization.

3.2.1. Fourier transformed infrared spectroscopy (FTIR)

IR spectra of AFC, PVP K_{30}, Na_2Co_3, PMs and optimized AA-AFC-SDs are shown in (**Error! Reference source not found.**) Pure AFC showed in distinct peaks at 3318 cm^{-1} (N–H $^{-1}$ stretching), 2935 cm^{-1} (O–H stretching), and the peak 1771 cm^{-1} (O–H stretching). C–O stretching is allocated 1717 cm^{-1}, band 1584 cm^{-1} (aromatic C– C stretching skeleton vibration), 1507 cm^{-1} (N–H in plane bending), 1344 cm^{-1} (O–H in plane bending), 1287 cm^{-1} (C–N aromatic amine), 963 cm^{-1} (O–H out plane bending), and 749 cm^{-1} (aromatic C– C stretching skeleton vibration) [26]. FTIR Spectrum of PVP K30 had a characteristic absorption band at 1655 cm^{-1} for carbonyl group is responsible for this. The presence of moisture can be seen in the very wide band at 3447 cm^{-1}, indicating that PVP K30 is hygroscopic [46, 47]. Na_2Co_3 showed a characteristic peak at 693 ,871,1443 ,1777 [48]. The FTIR spectrum of HPβCD showed a wide absorption band at 3423 cm^{-1}. Other notable peaks included those at 2931 cm^{-1} (for C-H stretching vibrations) and bands between 1384 and 1460 cm^{-1} (for CH_2 and CH_3 bending vibrations) [49]. The presence of distinctive drug and carrier peaks in any PMs or SDs with no extra peaks can rule out any drug-carrier interaction, implying these systems have AFC stability [27].

3.2.2. Differential scanning calorimetry

DSC thermograms of AFC, PVP K30, Na_2Co_3, PMs and AA-AFC-SDs were represented in (**Error! Reference source not found.**). Thermogram of pure AFC revealed strong peaks at 152°C and 275°C, respectively, indicating the melting point and polymorphic nature of AFC [50]. The first endothermic peak in the DSC thermogram of PVP K30 is at 100 °C, which attributed to the glass transition temperature, then a deep endothermic peak developed at 400 °C, indicating thermal breakdown [51]. Na_2Co_3 thermogram shows a characteristic peak at 90–110°C, the influence of residual moisture in Na_2CO_3 is likely to be the reason [52]. According to the DSC thermogram of HPβCD the dehydration temperature was 60°C [52]. And melting was recorded at 340°C [53]. The reduction of the drug peak in both PMs is due to carrier dilution, simultaneously, AFC endothermic peaks vanished from DSC curves of SDs with PVP K_{30} and HPβCYD. Indicating amorphization of AFC by SD formation [27].

3.2.3. X-ray diffractometry

As seen by multiple peaks (**Error! Reference source not found.**) at 8.7, 11.5, 14.5, 16.8, 17.5, 18.4, 19.4, 22.2, 24.41, 25.9, 26.4, 32.1, and 36.5. The diffraction pattern of pure AFC was highly crystalline [22, 47]. Because PVP K30 is an amorphous polymer, no sharp peak was observed [30, 54]. After $30^{O}C$, Na_2CO_3 revealed variety of sharp and high-intensity peaks, demonstrating its crystalline character [17]. X-ray diffraction peaks of HPβCYD indicate its amorphization [55]. The intensity of drug peaks is reduced in PMs of AFC with each carrier and alkalizer, perhaps due to dilution by the carriers. Diffractograms of SDs showed either a considerable reduction or the disappearance of AFC peaks when compared to the comparable PMs, presumably showing the drug's amorphization or reduced crystallinity. There were no new peaks identified in the PMs and SDs that were investigated, showing that there was no interaction between the drug and the carriers used, as confirmed by FTIR and DSC data [27].

3.2.4. Scanning electron microscopy

The surface morphologies of pure AFC, PVP K 30, HPβCYD, each PM and SD were determined by SEM as shown in (Figure 2). Pure AFC was found to have a crystalline appearance [(9)]. Na_2CO_3 and PVP K 30 were seen as irregular fragments and round-shaped particles, respectively [47]. The HPβCYD particles have large size, rough surfaces and irregularly shaped [55]. All PMs drug crystals were found with irregular fragments of Na_2Co_3 and with round shaped particles of PVP K30 in PM3 and irregularly shaped rough surfaces particles of HPβCYD in PM9. Unlike pure AFC, SDs formulation revealed one kind of amorphous particle with a morphology distinct in the surface. This revealed that all of the ingredients were evenly dispersed throughout the preparations, resulting in the formation of the SDs, which could be the cause of AFC's higher dissolution rate. DSC thermograms verified these findings [27].

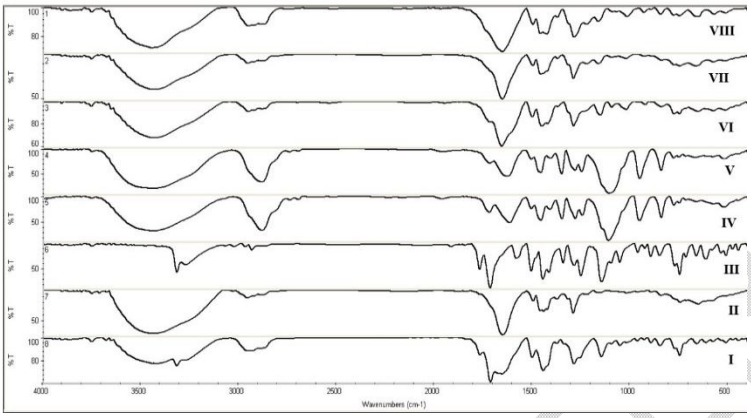

A

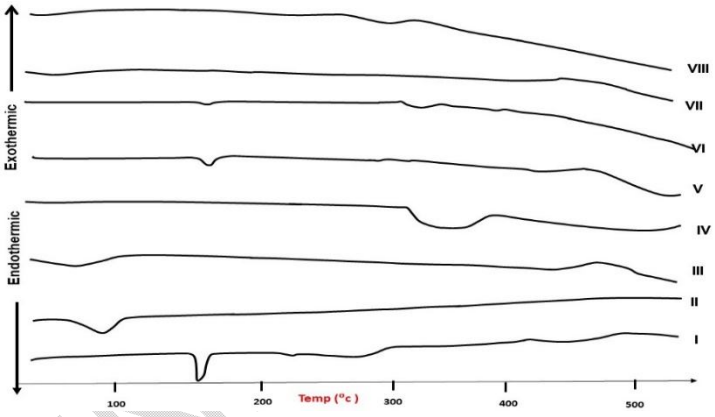

B

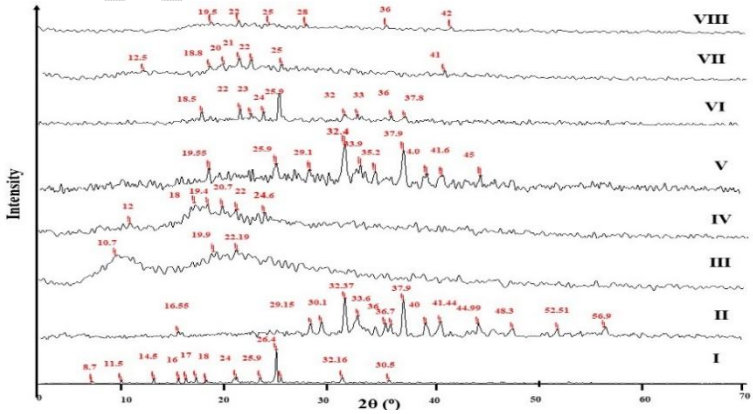

Figure 1: Solid characterizations

***Notes**: 1(A) ATR-FTIR spectra, 1(B) DSC and 3(C) XRD pattern curves of I) AFC, (II) Na2Co3, (III) PVP K30, (IV) HPβCYD, (V) PM3, (VI)PM9, (VII) SD3, (VIII) SD9.*

***Abbreviation:** AFC, aceclofenac; PVP K30 polyvinyl pyrrolidine K30; HPβCYD, hydroxy propyl beta cyclodextrin; PM, physical mixture; SD, solid dispersion, FTIR, Fourier transform infrared spectroscopy; DSC, differential scanning calorimetry; XRD, X-ray diffractometry.*

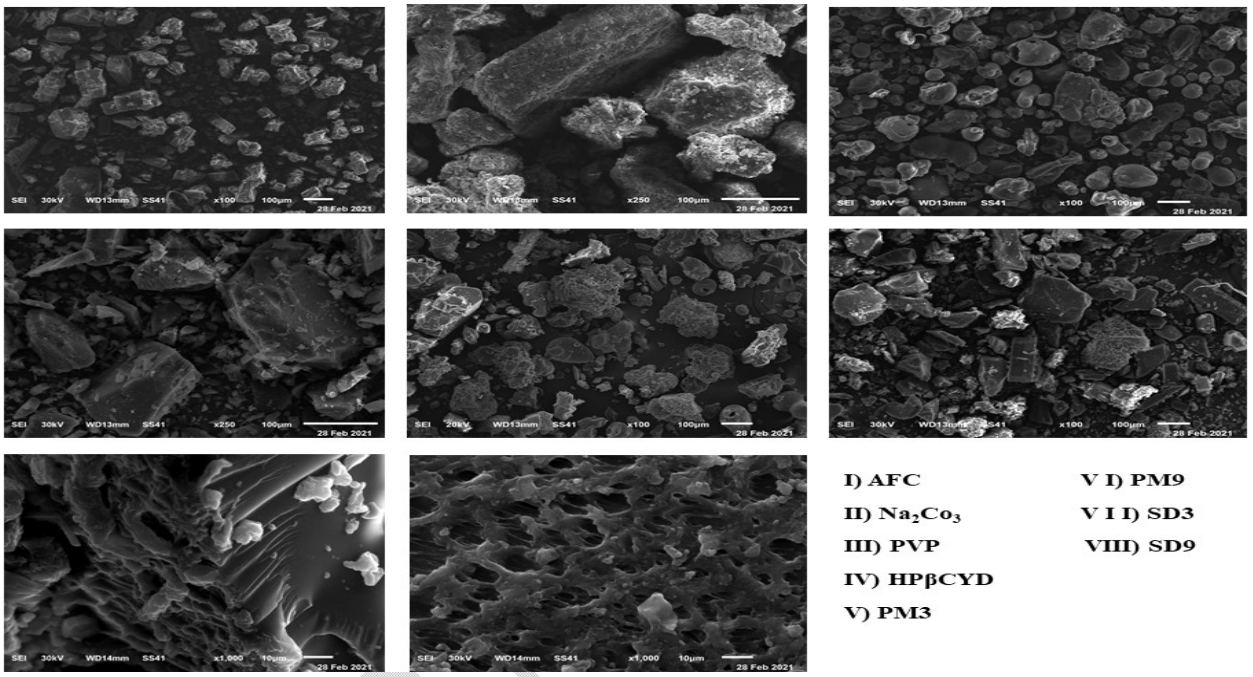

Figure 2: **Scanning electron microscopy.**

***Abbreviation**: AFC, aceclofenac; PVP K30, polyvinyl pyrrolidine K30; HPβCYD, hydroxy propyl beta cyclodextrin; PM, physical mixture; SD, solid dispersion.*

3.2.5. Drug content and Percentage yield

The results of drug content and percentage yield of all preparations were illustrated in Table 2. It's clear that the range of prepared solid dispersion with each carrier was 90.1 % ± 1.34: 100.09%±0.93, which met the pharmacopoeia limit of 90%: 110% [56].

Table 2: Drug content and percentage yield of the prepared ternary systems for each polymer

Preparation code	Polymer used	(Drug: Polymer Ratio)	Drug content	Percentage yield

SD1	PVP K30	1:1	94.1± 1.1	95.05 ± 2.23
SD2	PVP K30	1:3	95.8 ± 0.50	97.6 ±0.82
SD3	PVP K30	1:5	97±0.32	96.9 ±1.27
SD4	PEG 6000	1:1	90.5±1.64	74.32±1.45
SD5	PEG 6000	1:3	90.1 ± 1.34	78.75±3.19
SD6	PEG 6000	1:5	91.9 ± 1.25	82.9 ±3.22
SD7	HPβCYD	1:1	97.31±0.24	93.39 ±1.06
SD8	HPβCYD	1:3	97.5± 0.26	95.84±0.55
SD9	HPβCYD	1:5	100.09±0.93	95.8 ± 0.97

3.3. In-vitro dissolution behavior of different Preparations:

As highlighted in figure 3 In-vitro dissolution of the drug as SD with PVP K30 compared to the unprocessed powder, led in a considerable increase in the drug's dissolving rate (**Error! Reference source not found.**). This increase in dissolving rate was dependent on the polymer concentration as the dissolution rate was increased concurrently with the increase in the polymer concentration [31, 46]. The dissolution rate of drug was increased by the ternary mixtures in the form of PMs. This effect was less pronounced than in the case of SDs. The wetting effect of the polymer can be attributed to the observed effect in the case of physical mixtures, on the other hand, enhanced dissolution in the case of SD was due to a possible physical change in the crystalline structure [46].

In the case of PEG 6000 Figure3B preparing SD with the drug resulted in a gradual increase in the dissolving rate at low polymer concentrations, with the amount of drug dissolved in the first 10 minutes being 46% in 1:1 (drug to polymer, weight ratios). In the instance of the 1:3 and 1:5 SD, this amount grew dramatically, reaching ˙ 79% [46, 54]. In case of HPβCYD (**Error! Reference source not found.**) increasing concentration of the polymer result in an increase of dissolution rate. Similar dissolution behavior has been reported [57]. Physical mixing of the drug with each polymer and the selected alkalizer at all ratios, increased drug release significantly compared to the drug alone (**Error! Reference source not found.** A, B and C). AA-AFC-SD formulations, which led in considerably greater drug release than the drug alone and equivalent PMs. Therefore, it can be said that AFC in vitro release was dependent on the ternary system being significantly higher in the case of AA-AFC-SDs, as was indicated by the significantly higher average values of DE30 of these systems relative to those of corresponding PMs as shown in Table 3. RDR_{30} readings calculated at the same time reflected this behavior. The higher drug dissolution on SDs with AFC than combining with either carrier physically may have confirmed reduction in crystallinity or full amorphization of the drug, as indicated by DSC, XRD, and SEM results (Figure 1-2). An amorphous drug is predicted to disintegrate faster than a crystalline form, because of its high energy [33, 34].

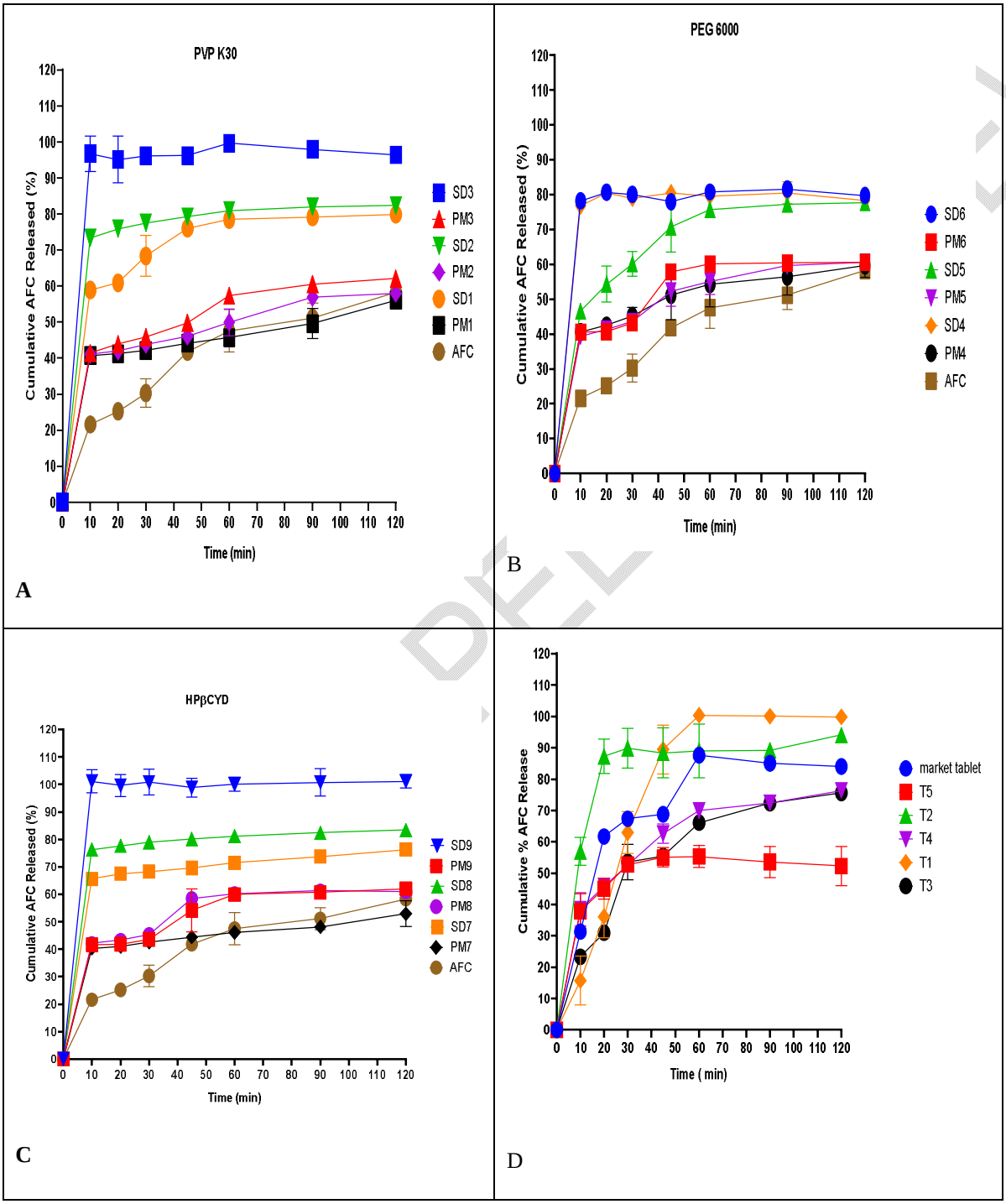

Figure 3 *:* **Dissolution study in Phosphate buffer pH 6.**

Notes*: (A) PVP K30 SDs and PMs, (B) PEG6000 SDs and PMs, and (C) HPβCYD SDs and PMs (D)Tablet dissolution.*

***Abbreviation**: AFC, aceclofenac; PVP K30 polyvinyl pyrrolidine K30; HPβCYD, hydroxy propyl beta cyclodextrin; PEG 6000, polyethylene glycol 6000; PM, physical mixture; SD, solid dispersion*

Table 3: Dissolution efficiency (DE) and relative dissolution rate (RDR) of AFC ternary systems

Formulation code	Dissolution parameter		
	$DE_{30\ min}$ (mean ± SD), n=3	Fold increase	$RDE_{30\ min}$
AFC	18.36	----	----
PVP K30			
PM1	34.34 [a]	1.51	4.40
PM2	34.99 [a]	1.57	4.26
PM3	36.10 [a]	1.64	4.20
SD1	51.33 [a, c]	2.45	6.09
SD2	62.68 [a,c,d]	2.78	6.51
SD3	80.00 [a,c,d]	3.45	7.01
PEG 6000			
PM4	35.27 [a]	1.62	8.94
PM5	34.18 [a]	1.57	9.06
PM6	34.31 [a]	1.55	7.68
SD4	43.68 [a,c]	2.16	4.12
SD5	60.79 [a,c,d]	2.92	4.28
SD6	60.79 [a,c,d]	2.87	4.13
HPβCYD			
PM7	35.27 [a]	1.53	7.01
PM8	34.18 [a]	1.63	6.51
PM9	34.31 [a]	1.56	6.09
SD7	55.77 [a,c]	2.45	7.68
SD8	64.50 [a,c,d]	2.83	6.51
SD9	83.17 [a,c]	3.62	7.01

Notes: *[a] in comparison to AFC, [b] in comparison to 1:1 PM with similar carrier, [c] in comparison to the matching PM with similar carrier, [d] in comparison to 1:1 SD with similar carrier.*

3.4. Micromeritic Study

The results showing that all of the produced formulations had acceptable Micromeritic properties, making them appropriate for tablet compression as shown in Table 4

Table 4: **Physical properties of the powder blend of F1 and F2.**

Formula code	Angle of repose	Bulk density	Tapped density	Hausner's ratio	Carr's index
F1	39.81 ± 1.17	0.44±0.006	0.54±0.009	1.11±0.02	18.5±0.84
F2	37.55±1.07	0.26±0.007	0.30±0.007	1.19±0.05	13.33±3.62

***Note**: F1 and F2 are the powder blend before compression into tablet which consists of (SD3 and MCC for F1 or SD9 and MCC for F2).*

3.5. Tablet evaluation

Table 5 shows all prepared tablets physical parameters, it's important to note that all of the manufactured tablets met USP 40 standards for weight variation, thickness, hardness, friability, and drug content [36].

Table 5: Evaluation of AA-AFC SDs containing tablets

Formula code	thickness	diameter	hardness	friability	Drug content	Tablet weight
T1	4.45±0.05	12.19± 0.03	6.25±0.52	0.44±0.25	97.46±2.40	456±0.78
T2	4.15±0.02	12.04±0.02	8.75±0.75	1.01±0.11	100.9±1.42	442.5±0.95
T3	4.45±0.05	12.13±0.05	7.00±0.52	0.13±0.14	95.16±.40	456±0.18
T4	4.50±0.12	12.01±0.01	9.00±0.05	0.98±0.81	98.46±1.40	442.5±15
Market	3.53±0.001	8.05±0.001	9.25±0.005	0.001±0.01	99.9±.02	0.212±10

***Note:** The data is presented as mean ± SD*

3.5.1. In-vitro release

The dissolution profiles of AFC from AA-AFC SDs containing tablets, tablets containing PM, commercial tablet and free drug containing one are indicated in (**Error! Reference source not found.** was evaluated in phosphate buffers of pH 6.8. In comparison to the commercial or free drug containing tablets, the drug release from AA-AFC SDs containing tablets showed substantial difference after 2 hours of release. Commercial tablet showing an 84% drug release. The level of dissolution was in the order AA-AFC PVP K_{30} tablet > AA-AFC HPβCYD tablet > Market tablet > PM containing HPβCYD tablet > PM containing PVP K30 tablet > free drug containing tablet.

3.5.2. Kinetics release

Kinetic study is applied in the burst-release phase of AFC from ternary system. The findings showed that the mechanism for releasing AFC from these systems fluctuated between first- and zero-order kinetics throughout the burst-release phase (r^2 > 0.875). Therefore, the Korsmeyer–Peppas model was applied to verify the release mechanism. Supercase II transport, which relates to the degradation of polymer chains and describes the initial burst release, was suggested by release exponent (n) values larger than unity in T1 and T2 formulation [27]. All of the samples had a release exponent (n) in the range of 0.5826-0.9388, indicating non-Fickian drug release pattern combining drug diffusion through the carrier and carrier erosion [58].

3.5.3. Stability study

The key issues that determine the design of any dosage form are the drug's solubility and stability. During the six-month storage term of the stability investigation, the tablets of the selected formulae T1 and T2 were stable with no significant changes in their physical properties, drug content, or in-vitro drug release [36].

3.5.4. Anti-inflammatory properties against carrageenan-induced rat paw edema.

Figure 4 (A & B) shows edema lasting up to 24 hrs. & suppression of edema in groups given 10 mg/kg AFC only (free drug containing tablet (T5) or an equal dose of the two optimal AA-AFC-SDs containing tablet (T1&T2) and market one. All groups given drug alone (T5), two optimal formulations (T1&T2) and market one display remarkable decrease in edema in comparison to positive control group (Figure 4A). Animals given two optimal formulations (T1 & T2) present notable less edema than with the groups treated with drug alone. Rats given market tablet also show decrease in edema but it was less than the two optimal formulations.

Correlate well with in vitro release data. Up to 24 hours, edema inhibition in groups treated with either optimal T1 or T2 was generally higher than in those treated with market tablet and AFC alone **(**Figure 4B). The amorphous AFC particles allowing improved in vitro release and hence enhanced absorption may explain the advantage of the optimized formulae over free AFC in terms of anti-inflammatory action against carrageenan-induced rat paw edema [27, 59].

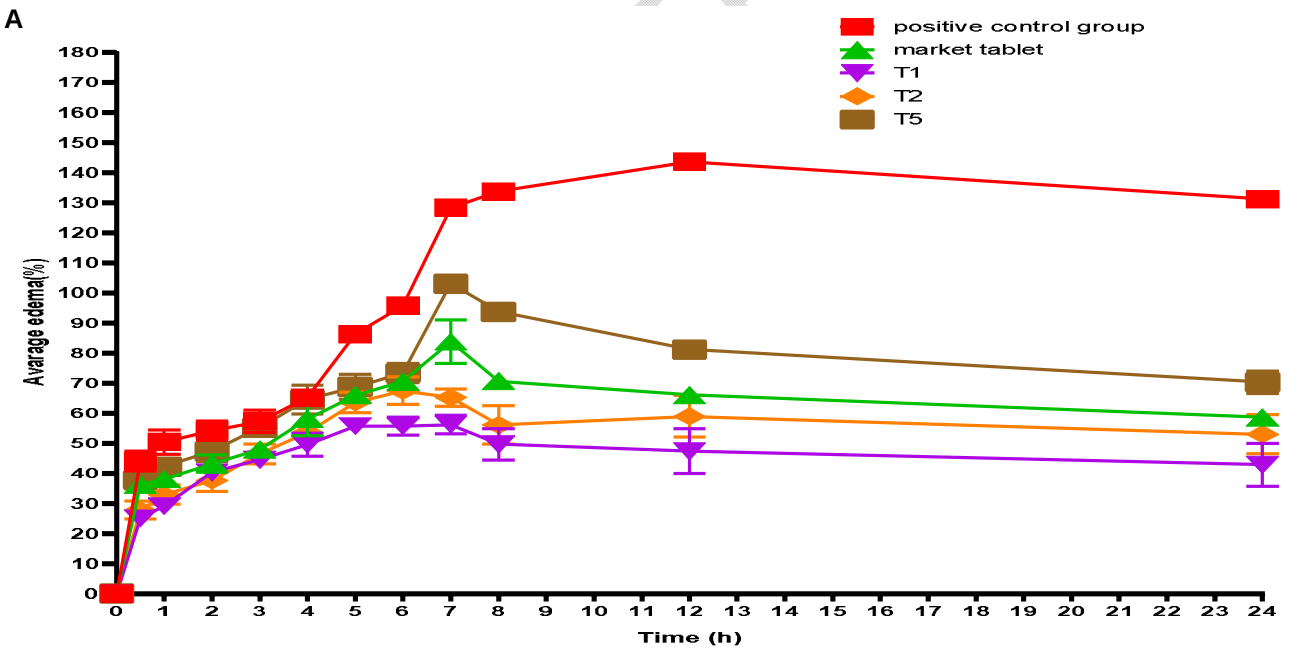

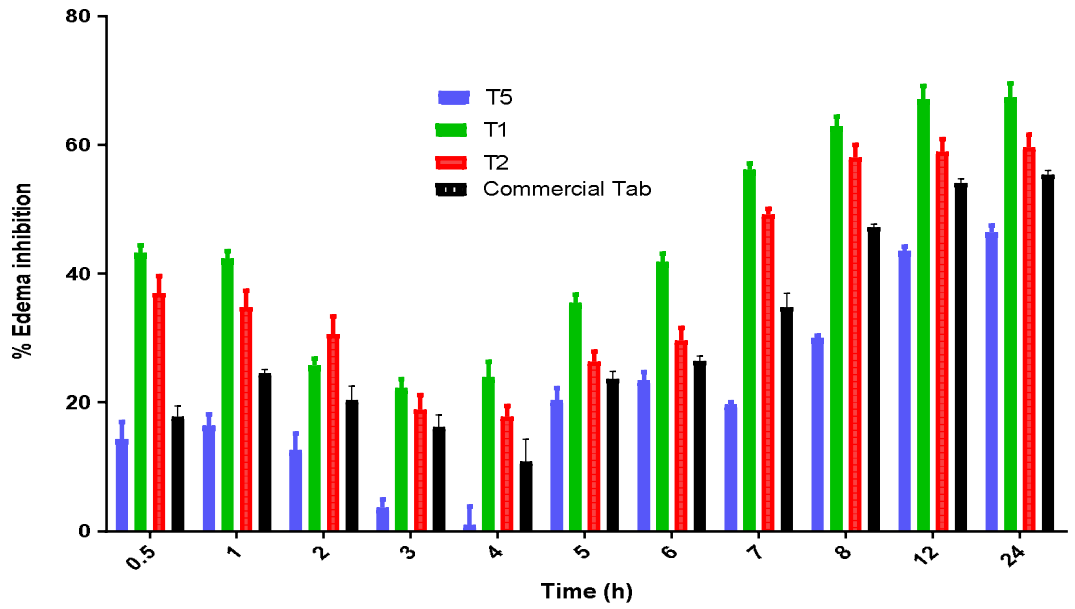

Figure 4: Edema and edema suppression in groups given 10 mg/kg AFC orally or a dose equal to the two optimal AA-AFC-SDs containing tablet in comparison with the positive carrageenan group.

3.5.5. Histopathological examination

As shown in (Figure 5) microscopic pictures of H&E stained thin and thick skin sections showing normal epidermal and dermal structures in normal group (I) X:100 bar 100. Microscopic pictures of H&E-stained skin sections from +ve control group (II) showing diffuse epidermal vacuolation (black arrows), severe and deep dermal inflammation (*) with congestion (red arrow) in thin skin, less severe dermal inflammation (*) with dilated blood vessels in thick skin (red arrows). Skin sections from group received free drug (III) showing decreased intensity of dermal inflammation (*) and congestion (red arrow) in both thin and thick skin when compared with control +ve group. Skin sections from groups received market drug (IV) showing focal epidermal vacuolation (black arrows), moderate degree of dermal inflammation (*) and congestion (red arrow) in both thin and thick skin when compared with control +ve group. Skin sections from AA-AFC-SDs containing tablets groups (VI, V respectively) showing mild degree of dermal inflammation (*) with subside of vascular reaction in both thin and thick skin. X:100 bar 100.

Figure 6 indicated the statistical analysis of inflammation scores in both thin and thick sections shows significant increase in control +ve when compared with normal group and significant reduction in groups pretreated with AA-AFC-SDs containing tablets when compared with control +ve group. Different symbols mean significant when $P<0.05$.

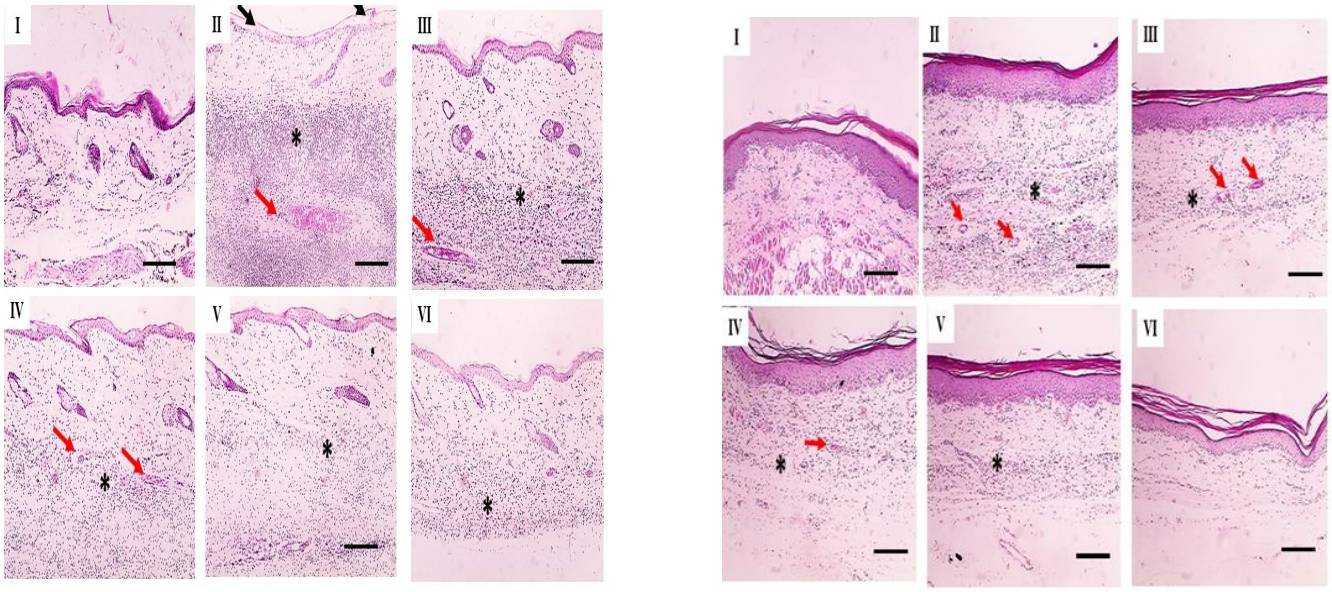

Figure 5*:* Histological examination (H&E, 100×) of rat paw skin.

Notes*: (A Microscopic picture of H&E-stained thin Skin and B thick skin sections) showing normal epidermal and dermal structures in normal group (I). Microscopic pictures of H&E-stained skin sections from control +ve group (II) showing diffuse epidermal vacuolation (black arrows), severe and deep dermal inflammation (*) with congestion (red arrow) in thin skin, less severe dermal inflammation (*) with dilated blood vessels in thick skin (red arrows). Skin sections from group received drug (III) showing decreased intensity of dermal inflammation (*) and congestion (red arrow) in both thin and thick skin when compared with control +ve group. Skin sections from market group (IV) showing focal epidermal vacuolation (black arrows), moderate degree of dermal inflammation (*) and congestion (red arrow) in both thin and thick skin when compared with control +ve group. Skin sections from AA-AFC-SDs containing tablets groups (V) &(VI) showing mild degree of dermal inflammation (*) with subside of vascular reaction in both thin and thick skin. X:100 bar 100.*

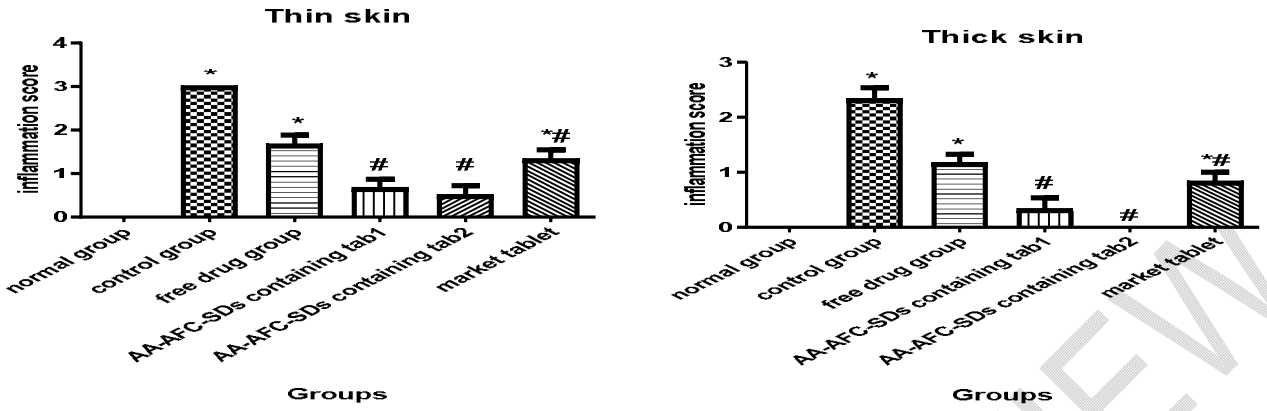

Figure 6: Statistical analysis of inflammation scores (non-parametric data so analyzed by Kruskal-Wallis test followed by Dunn's test) in both thin and thick sections shows significant increase in control +ve when compared with normal group and significant reduction in groups preatreated with AA-AFC-SDs containing tablets when compared with control +ve group. Different symbols mean significant when *P*<0.05.

CONCLUSION

In this research work, amorphous alkalinized aceclofenac solid dispersions were successfully formulated using solvent evaporation method that was free from any organic solvent. In comparison with pure AFC and corresponding PMs, significantly enhanced in vitro drug release was recorded for AA-AFC-SDs with either PVP K30 or HPβCYD. The optimal systems were 1:5 (AFC: PVP K30) and 1:5 (AFC: HPβCYD) since they show the highest drug release profiles. Characterization of solid state by FTIR, SEM, DSC and XRD confirmed transformation of crystalline form of drug into amorphous one with no drug-polymers interactions. AA-AFC-SDs containing tablets were simply prepared by direct compression with MCC. The dissolution behavior of selected tablets, was superior to that of Bristaflam (the commercial product). Stability study confirmed that the optimal tablets can satisfy the demand of formulation development. Moreover, anti-inflammatory activity against carrageenan induced paw edema indicated that the SD is a promising approach to enhance the dissolution rate and oral bioavailability of AFC.

From the studies, we concluded that a ternary solid dispersion approach of AFC can be successfully used to improve the dissolution and possibly bioavailability of poorly water-soluble AFC in a simple and economic manner. The studies also offered promising oral solid dosage form after scaling up the formulation in order to be potential commercial oral dosage form of AFC superlative to marketed formulation Bristaflam.

ETHICS APPROVAL AND CONSENT TO PARTICIPATE

Animal protocol was accepted by the ethical committee of Mansoura University's Faculty of pharmacy, Mansoura, Egypt, in accordance with “principles of laboratory animal care NIH publication revised 1985” **(Code number: 2022-179)**

REFERENCES

1. Loftsson T, Brewster ME. Pharmaceutical applications of cyclodextrins: basic science and product development. J Pharm Pharmacol. 2010;62(11):1607-21.
2. Chaumeil JC. Micronization: a method of improving the bioavailability of poorly soluble drugs. Methods and findings in experimental and clinical pharmacology. 1998;20(3):211-5.
3. Rasenack N, Muller BW. Micron-size drug particles: common and novel micronization techniques. Pharm Dev Technol. 2004;9(1):1-13.
4. Patel BB, Patel JK, Chakraborty S, Shukla D. Revealing facts behind spray dried solid dispersion technology used for solubility enhancement. Saudi Pharm J. 2015;23(4):352-65.
5. Feeney OM, Crum MF, McEvoy CL, Trevaskis NL, Williams HD, Pouton CW, et al. 50years of oral lipid-based formulations: Provenance, progress and future perspectives. Adv Drug Deliv Rev. 2016;101:167-94.
6. Crestani de Miranda J MT, Veiga F, Ferraz HG . Cyclodextrins and ternary complexes: technology to improve solubility of poorly soluble drugs. Braz J Pharm Sci (2011);47(4): 665-681.
7. Agrawal AM, Dudhedia MS, Zimny E. Hot Melt Extrusion: Development of an Amorphous Solid Dispersion for an Insoluble Drug from Mini-scale to Clinical Scale. AAPS PharmSciTech. 2016;17(1):133-47.
8. Dwayne T. Friesen, † Ravi Shanker,‡ Marshall Crew,†,§ Daniel T. Smithey,†,§ W. J. Curatolo,‡ and J. A. S. Nightingale†. Hydroxypropyl Methylcellulose Acetate Succinate-Based Spray-Dried Dispersions: An Overview. MOLECULAR PHARMACEUTICS. 2008.
9. Narayan R, Pednekar A, Bhuyan D, Gowda C, Koteshwara KB, Nayak UY. A top-down technique to improve the solubility and bioavailability of aceclofenac: in vitro and in vivo studies. Int J Nanomedicine. 2017;12:4921-35.
10. Dua K, Pabreja K, Ramana MV, Lather V. Dissolution behavior of beta-cyclodextrin molecular inclusion complexes of aceclofenac. J Pharm Bioallied Sci. 2011;3(3):417-25.
11. Damian F, Harati M, Schwartzenhauer J, Van Cauwenberghe O, Wettig SD. Challenges of Dissolution Methods Development for Soft Gelatin Capsules. Pharmaceutics. 2021;13(2).
12. Liu H, Taylor LS, Edgar KJ. The role of polymers in oral bioavailability enhancement; a review. Polymer. 2015;77:399-415.
13. Zhong L, Zhu X, Yu B, Su W. Influence of alkalizers on dissolution properties of telmisartan in solid dispersions prepared by cogrinding. Drug Development and Industrial Pharmacy. 2014;40(12):1660-9.
14. Tran PH, Tran HT, Lee BJ. Modulation of microenvironmental pH and crystallinity of ionizable telmisartan using alkalizers in solid dispersions for controlled release. Journal of controlled release : official journal of the Controlled Release Society. 2008;129(1):59-65.
15. Chae JS, Chae BR, Shin DJ, Goo YT, Lee ES, Yoon HY, et al. Tablet Formulation of a Polymeric Solid Dispersion Containing Amorphous Alkalinized Telmisartan. AAPS PharmSciTech. 2018;19(7):2990-9.
16. Alshehri S, Imam SS, Hussain A, Altamimi MA, Alruwaili NK, Alotaibi F, et al. Potential of solid dispersions to enhance solubility, bioavailability, and therapeutic efficacy of poorly water-soluble drugs: newer formulation techniques, current marketed scenario and patents. Drug Deliv. 2020;27(1):1625-43.
17. Marasini N, Tran TH, Poudel BK, Cho HJ, Choi YK, Chi SC, et al. Fabrication and evaluation of pH-modulated solid dispersion for telmisartan by spray-drying technique. International journal of pharmaceutics. 2013;441(1-2):424-32.
18. Yamashita K, Nakate T, Okimoto K, Ohike A, Tokunaga Y, Ibuki R, et al. Establishment of new preparation method for solid dispersion formulation of tacrolimus. International journal of pharmaceutics. 2003;267(1-2):79-91.
19. Park J, Cho W, Cha KH, Ahn J, Han K, Hwang SJ. Solubilization of the poorly water soluble drug, telmisartan, using supercritical anti-solvent (SAS) process. International journal of pharmaceutics. 2013;441(1-2):50-5.
20. Qian F, Huang J, Hussain MA. Drug-polymer solubility and miscibility: Stability consideration and practical challenges in amorphous solid dispersion development. Journal of pharmaceutical sciences. 2010;99(7):2941-7.
21. Xu S, Dai WG. Drug precipitation inhibitors in supersaturable formulations. International journal of pharmaceutics. 2013;453(1):36-43.
22. Patnaik S, Aditha SK, Rattan T, Kamisetti V. Aceclofenac-Soluplus: Nanocomposites for Increased Bioavailability. Soft Nanoscience Letters. 2015;05(02):13-20.
23. Kang WH, Nguyen HV, Park C, Choi YW, Lee BJ. Modulation of microenvironmental pH for dual release and reduced in vivo gastrointestinal bleeding of aceclofenac using hydroxypropyl methylcellulose-based bilayered matrix tablet. Eur J Pharm Sci. 2017;102:85-93.
24. Maulvi FA, Dalwadi SJ, Thakkar VT, Soni TG, Gohel MC, Gandhi TR. Improvement of dissolution rate of aceclofenac by solid dispersion technique. Powder Technology. 2011;207(1-3):47-54.
25. Park JJ, Meghani N, Choi JS, Lee BJ. Development and evaluation of decorated aceclofenac nanocrystals. Colloids Surf B Biointerfaces. 2016;143:206-12.

26. Rahim H, Sadiq A, Ullah R, Bari A, Amin F, Farooq U, et al. Formulation of Aceclofenac Tablets Using Nanosuspension as Granulating Agent: An Attempt to Enhance Dissolution Rate and Oral Bioavailability. Int J Nanomedicine. 2020;15:8999-9009.
27. Eltobshi AA, Mohamed EA, Abdelghani GM, Nouh AT. Self-nanoemulsifying drug-delivery systems for potentiated anti-inflammatory activity of diacerein. Int J Nanomedicine. 2018;13:6585-602.
28. Qushawy M, Nasr A, Swidan S, Mortagi Y. Development and Characterization of Glimepiride Novel Solid Nanodispersion for Improving Its Oral Bioavailability. Scientia Pharmaceutica. 2020;88(4).
29. Reginald-Opara JN, Attama A, Ofokansi K, Umeyor C, Kenechukwu F. Molecular interaction between glimepiride and Soluplus®-PEG 4000 hybrid based solid dispersions: Characterisation and anti-diabetic studies. International journal of pharmaceutics. 2015;496(2):741-50.
30. EL-NABARAW MA. Optimization of class II BCS drug using solid dispersion technique. International Journal of Pharmacy and Pharmaceutical Sciences. 2012.
31. Kim MJ, Lee J, Yoon H, Kim S, Jeon DY, Jang J, et al. Preparation, characterization and in vitro dissolution of aceclofenac-loaded PVP solid dispersions prepared by spray drying or rotary evaporation method. 2013;43:107-13.
32. Ahuja N, Katare OP, Singh B. Studies on dissolution enhancement and mathematical modeling of drug release of a poorly water-soluble drug using water-soluble carriers. Eur J Pharm Biopharm. 2007;65(1):26-38.
33. Mohamed EA, Meshali MM, Foda AM, Borg TM. Improvement of dissolution and hypoglycemic efficacy of glimepiride by different carriers. AAPS PharmSciTech. 2012;13(3):1013-23.
34. Abdelkader H AO, Salem HS. . Comparison of the effect of tromethamine and polyvinylpyrrolidone on dissolution properties and analgesic effect of nimesulide. . AAPS PharmSciTech.2007;8(3):E110–E117.
35. Teaima MH, Yasser M, El-Nabarawi MA, Helal DA. Proniosomal Telmisartan Tablets: Formulation, in vitro Evaluation and in vivo Comparative Pharmacokinetic Study in Rabbits. Drug Des Devel Ther. 2020;14:1319-31.
36. Awadeen RH, Boughdady MF, Meshali MM. New in-situ gelling biopolymer-based matrix for bioavailability enhancement of glimepiride; in-vitro/in-vivo x-ray imaging and pharmacodynamic evaluations. Pharm Dev Technol. 2019;24(5):539-49.
37. Yasser M, Teaima M, El-Nabarawi M, El-Monem RA. Cubosomal based oral tablet for controlled drug delivery of telmisartan: formulation, in-vitro evaluation and in-vivo comparative pharmacokinetic study in rabbits. Drug Dev Ind Pharm. 2019;45(6):981-94.
38. Georgy KR, Farid RM, Latif R, Bendas ER. A new design for a chronological release profile of etodolac from coated bilayer tablets: In-vitro and in-vivo assessment. J Adv Res. 2019;15:37-47.
39. Osman HF AA. Influence of electrolytes supplementation on cardiac and renal functions after prolonged exercise in male rats. World Appl Sci J 2013;23:1377–85. doi: https://doi.org/10.5829/idosi.wasj.2013.23.10.7522.
40. Mei Z, Li X, Wu Q, Hu S, Yang X. The research on the anti-inflammatory activity and hepatotoxicity of triptolide-loaded solid lipid nanoparticle. Pharmacological research. 2005;51(4):345-51.
41. Bancroft JD, Gamble M. Theory and practice of histological techniques. London; New York: Churchill Livingstone; 2002.
42. Riella KR, Marinho RR, Santos JS, Pereira-Filho RN, Cardoso JC, Albuquerque-Junior RL, et al. Anti-inflammatory and cicatrizing activities of thymol, a monoterpene of the essential oil from Lippia gracilis, in rodents. Journal of ethnopharmacology. 2012;143(2):656-63.
43. Sumana N, Chhitij T. Formulation and enhancement of dissolution rate of poorly aqueous soluble drug Aceclofenac by solid dispersion method: In vitro study. African Journal of Pharmacy and Pharmacology. 2020;14(1):1-8.
44. Tran TT-D, Tran PH-L, Lee B-J. Dissolution-modulating mechanism of alkalizers and polymers in a nanoemulsifying solid dispersion containing ionizable and poorly water-soluble drug. European Journal of Pharmaceutics and Biopharmaceutics. 2009;72(1):83-90.
45. Tran TT-D. Physicochemical principles of controlled release solid dispersion containing a poorly water-soluble drug. future-science. 2010.
46. El Maghraby GM, Elsergany RN. Fast disintegrating tablets of nisoldipine for intra-oral administration. Pharm Dev Technol. 2014;19(6):641-50.
47. Al-Japairai KAS, Alkhalidi HM, Mahmood S, Almurisi SH, Doolaanea AA, Al-Sindi TA, et al. Lyophilized Amorphous Dispersion of Telmisartan in a Combined Carrier-Alkalizer System: Formulation Development and In Vivo Study. ACS Omega. 2020;5(50):32466-80.
48. Kiefer J, Stärk A, Kiefer A, Glade H. Infrared Spectroscopic Analysis of the Inorganic Deposits from Water in Domestic and Technical Heat Exchangers. Energies. 2018;11(4).
49. Onyeji. CO, SIO, Oladimeji FA, Soyinka. JO. Physicochemical characterization and dissolution properties of binary systems of pyrimethamine and 2hydroxypropyl-□-cyclodextrin

2009.
50. Jana S, Ali SA, Nayak AK, Sen KK, Basu SK. Development of topical gel containing aceclofenac-crospovidone solid dispersion by “Quality by Design (QbD)” approach. Chemical Engineering Research and Design. 2014;92(11):2095-105.
51. Anwar M, Pervaiz F, Shoukat H, Noreen S, Shabbir K, Majeed A, et al. Formulation and evaluation of interpenetrating network of xanthan gum and polyvinylpyrrolidone as a hydrophilic matrix for controlled drug delivery system. Polymer Bulletin. 2020;78(1):59-80.
52. Giri BR, Kwon J, Vo AQ, Bhagurkar AM, Bandari S, Kim DW. Hot-Melt Extruded Amorphous Solid Dispersion for Solubility, Stability, and Bioavailability Enhancement of Telmisartan. Pharmaceuticals (Basel). 2021;14(1).
53. Tambe Amruta PN, Prashant S. Kharkar, Niteshkumar U. Sahu. Encapsulation of Boswellic acid with β- and Hydroxypropyl-β-Cyclodextrin: Synthesis, Characterization, In vitro Drug Release and Molecular Modelling Studies Journal of Molecular Structure. 2017.
54. Dos Santos KM, Barbosa RM, Vargas FGA, de Azevedo EP, Lins A, Camara CA, et al. Development of solid dispersions of beta-lapachone in PEG and PVP by solvent evaporation method. Drug Dev Ind Pharm. 2018;44(5):750-6.
55. Yousaf AM, Qadeer A, Raza SA, Chohan TA, Shahzad Y, Din FU, et al. Influence of levodropropizine and hydroxypropyl-beta-cyclodextrin association on the physicochemical characteristics of levodropropizine loaded in hydroxypropyl-beta-cyclodextrin microcontainers: Formulation and in vitro characterization. Polim Med. 2019;49(1):35-43.
56. B. P. British Pharmacopeia.;Vol. III.(The Stationary Office; 2010.):pp. 3155–7.
57. Mahapatra. AK, P. PNMA, Mahapatra. K, SB, and Siba P. Pradhan. Dissolution Enhancement and Physicochemical Characterization of Valsartan in Solid Dispersions with β-CD, HP β-CD, and PVP K-30. 2011.
58. Md. Zahir Uddin JAC, Ikramul Hasan and Md. Selim Reza. Enhancement of Dissolution Profile of Poorly Water Soluble Loratadine by Solid Dispersion Technique. 2016.
59. Fouad SA, Malaak FA, El-Nabarawi MA, Abu Zeid K. Development of orally disintegrating tablets containing solid dispersion of a poorly soluble drug for enhanced dissolution: In-vitro optimization/in-vivo evaluation. PLoS One. 2020;15(12):e0244646.